

## Supporting Information

### High-resolution NMR Spectroscopy for Measuring Complex Samples Based on Chemical-shift-difference Selection

Ziqiao Chen, Xueting Li, Yuqing Huang, Shuohui Cao, Zhong Chen, Yulan Lin\*

Department of Electronic Science, Fujian Provincial Key Laboratory of Plasma and Magnetic  
Resonance, State Key Laboratory of Physical Chemistry of Solid Surfaces, Xiamen University,  
Xiamen, China

\* Corresponding author.

Email: yulan.lin@xmu.edu.cn

#### Table of Content

1. Detailed signal evolution for CHEESE pulse sequence
2. Experimental details
3. Chemical shifts and  $J$ -coupling constants of coupled protons in D-fructose
4. Spectral foldings in CHEESE experiment
5. *Spinach* codes of performing CHEESE experiment on D-fructose
6. Pulse program codes for Varian spectrometers

## 1. Detailed signal evolution for CHEESE pulse sequence

Herein, we use polarization operators to deduce the coupled spins evolution on the action of the CHEESE sequence (Fig.1). The CHEESE experiment can be simplified to the following model:

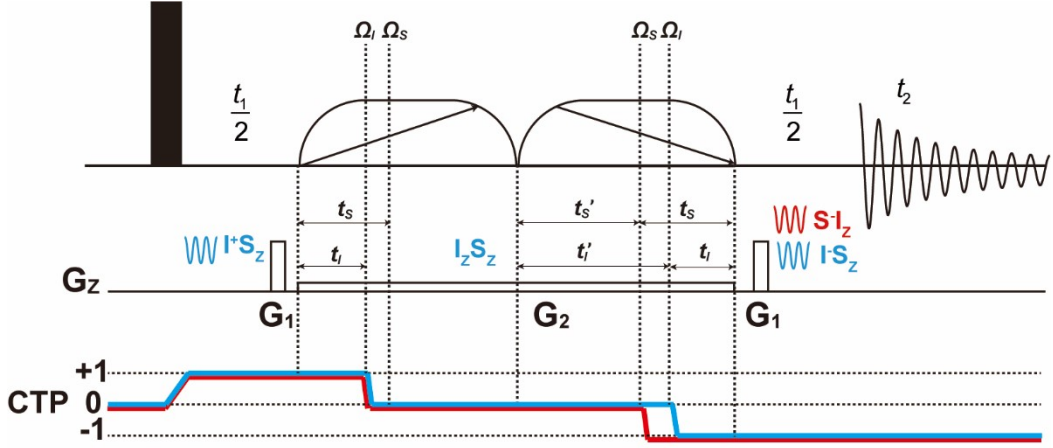


**Figure S1.** The simplified model for CHEESE experiment. Black rectangle represents non-selective  $90^\circ$  pulse. Trapezoids with diagonal arrows are low-power frequency-swept chimp pulses of net flip angle  $\theta = 15^\circ$ , the direction of frequency sweep for both chimp pulses are opposed as indicated by arrows.  $G_1$  and  $G_2$  are field gradient pulses.

Taking a two-spin weakly coupled system  $IS$  as an example, where  $I$  and  $S$  are active and passive spins respectively.  $\Omega_I$  and  $\Omega_S$  are chemical shifts of spins  $I$  and  $S$  respectively,  $J_{IS}$  is the coupling constant between spins  $I$  and  $S$ . The nonselective  $90^\circ$  pulse generates in-phase magnetization along the  $y$ -axis,  $-\hat{I}_y$  and  $-\hat{S}_y$ , which are shorthands for  $-\hat{I}_y\hat{U}_I$  and  $-\hat{S}_y\hat{U}_S$  respectively in terms of polarization operators. Here  $\hat{I}_y = \frac{1}{2i}(\hat{I}^+ - \hat{I}^-)$ ,  $\hat{S}_y = \frac{1}{2i}(\hat{S}^+ - \hat{S}^-)$ ,  $\hat{U}_I = \hat{I}_\alpha + \hat{I}_\beta$ ,  $\hat{U}_S = \hat{S}_\alpha + \hat{S}_\beta$ . [1] Substituting in these expressions gives

$$-\hat{I}_y - \hat{S}_y = -\frac{1}{2i} \left( \hat{I}^+ \hat{S}_\alpha + \hat{I}^+ \hat{S}_\beta - \hat{I}^- \hat{S}_\alpha - \hat{I}^- \hat{S}_\beta + \hat{S}^+ \hat{I}_\alpha + \hat{S}^+ \hat{I}_\beta - \hat{S}^- \hat{I}_\alpha - \hat{S}^- \hat{I}_\beta \right) \quad (S1)$$

Only terms containing  $\hat{I}^+$  and  $\hat{S}^+$  will be selected to evolve along the coherence transfer pathway (CTP). For simplicity, only the term  $\hat{I}^+ \hat{S}_\alpha$  is deduced in detail. The derivation of other terms is similar. The

free precession Hamiltonian  $\hat{H}_{FP}$  in weakly coupled system can be expressed as [2]

$$\hat{H}_{FP} = \Omega_I \hat{I}_z + \Omega_S \hat{S}_z + \pi J_{IS} 2\hat{I}_z \hat{S}_z \quad (\text{S2})$$

For a weakly coupled two-spin system, the basis functions ( $|\alpha\alpha\rangle, |\alpha\beta\rangle, |\beta\alpha\rangle, |\beta\beta\rangle$ ) are eigenfunctions of the free precession Hamiltonian  $\hat{H}_{FP}$ . The elements of the density matrix  $\hat{\rho}_{ij}$  evolve according to the following rule[2]:

$$\hat{\rho}_{ij}(t) \xrightarrow{\hat{H}_{FP}t} \hat{\rho}_{ij}(0) \exp\left[i(\hat{E}_j - \hat{E}_i)t\right]$$

where  $\hat{E}_i$  are the energies of the corresponding basis functions, listed below:

<i>Energy</i>	<i>Basis function</i>
$\hat{E}_1 = \frac{1}{2}(\Omega_I + \Omega_S + \pi J_{IS})$	$ \alpha\alpha\rangle$
$\hat{E}_2 = \frac{1}{2}(\Omega_I - \Omega_S - \pi J_{IS})$	$ \alpha\beta\rangle$
$\hat{E}_3 = \frac{1}{2}(-\Omega_I + \Omega_S - \pi J_{IS})$	$ \beta\alpha\rangle$
$\hat{E}_4 = \frac{1}{2}(-\Omega_I - \Omega_S + \pi J_{IS})$	$ \beta\beta\rangle$

The term  $\hat{I}^+ \hat{S}_\alpha$  represents  $\hat{\rho}_{13}$ , which evolves at frequency  $\hat{E}_3 - \hat{E}_1 = -(\Omega_I + \pi J_{IS})$ . During the first free evolution  $t_1/2$  period, the evolution of the coherence term  $\hat{I}^+ \hat{S}_\alpha$  can be presented as:

$$\hat{I}^+ \hat{S}_\alpha \xrightarrow{\hat{H}_{FP} \frac{t_1}{2}} \hat{I}^+ \hat{S}_\alpha \exp\left[-i(\Omega_I + \pi J_{IS}) \frac{t_1}{2}\right] \quad (\text{S3})$$

The key of the CHEESE technique is the PSYCHE element, the mechanism of chemical-shift-difference filtration is shown in Fig. S1. In PSYCHE element, the sweep frequency of a pair of chirp pulses is linearly with time in opposite direction. The sweep frequencies  $\omega_{1c}(t)$ ,  $\omega_{2c}(t)$  and the phases  $\phi_{1c}(t)$ ,  $\phi_{2c}(t)$  respectively

corresponding to the first and second chirp pulse are given by [3]

$$\begin{aligned}\omega_{1c}(t) &= O_i - Rt, & \phi_{1c}(t) &= \int_0^{t^{\max}-t} \omega_{1c}(\tau) d\tau = O_i(t^{\max}-t) - \frac{R}{2}(t^{\max}-t)^2 \\ \omega_{2c}(t) &= O_f + Rt, & \phi_{2c}(t) &= \int_0^{t^{\max}-t} \omega_{2c}(\tau) d\tau = O_f(t^{\max}-t) + \frac{R}{2}(t^{\max}-t)^2\end{aligned}\tag{S4}$$

where  $O_f = -O_i$ ,  $t^{\max} = 2O_i / R$ .  $O_i$  and  $O_f$  are the initial and final sweep frequency of the first chirp pulse, respectively.  $R$  is the sweep rate of the first chirp pulse. As the direction of the sweep frequency for both chirp pulses are opposite,  $O_i$  and  $O_f$  are the final and first sweep frequency of the second chirp pulse, respectively. In the action of the gradient field  $G_2$  along the  $z$ -axis, the spin with chemical shift  $\Omega$  is addressed by the first chirp pulse only when  $\omega_c(t) = \Omega + \gamma G_2 z$ . As shown in Fig. S1, spins  $I$  and  $S$  are addressed by the first chirp pulse at the end of the period  $t_I$  and  $t_S$  respectively, and are addressed by the second chirp pulse at the end of the period  $t'_I$  and  $t'_S$  respectively.

According to Eq. (S4), the time  $t_{I/S}$  and  $t'_{I/S}$ , as well as the phases  $\phi_{1c}(t_{I/S})$ ,  $\phi_{2c}(t'_{I/S})$  when the first and second chirp pulses act on spin  $I$  and spin  $S$  can be obtained,

$$\begin{aligned}t_{I/S} &= \frac{-(\Omega_{I/S} + \gamma G_2 z) + O_i}{R}, & \phi_{1c}(t_{I/S}) &= O_i(t^{\max} - t_{I/S}) - \frac{R}{2}(t^{\max} - t_{I/S})^2 \\ t'_{I/S} &= \frac{O_i + (\Omega_{I/S} + \gamma G_2 z)}{R}, & \phi_{2c}(t'_{I/S}) &= -O_i(t^{\max} - t'_{I/S}) + \frac{R}{2}(t^{\max} - t'_{I/S})^2\end{aligned}\tag{S5}$$

During the  $t_1 + \delta_1$  period, the coherence term  $\hat{I}^+ \hat{S}_\alpha$  evolves under the free precession Hamiltonian  $\hat{H}_{FP}$  and the gradient fields  $G_1$  and  $G_2$ , the coherence term is given by

$$Eq.(S3) \xrightarrow{\hat{H}_{FP}(t_I + \delta_1) + \gamma G_1 z \delta_1 + \gamma G_2 z t_I} \hat{I}^+ \hat{S}_\alpha e_1 \exp \left[ -i(\Omega_I + \pi J_{IS}) \frac{t_1}{2} \right] \quad (S6)$$

where

$$e_1 = \exp[-i(\Omega_I + \pi J_{IS})(t_I + \delta_1) - i\gamma G_1 z \delta_1 - i\gamma G_2 z t_I] \quad (S7)$$

and  $\delta_1$  is the duration of the gradient  $G_1$ . At the end of the  $t_1$  period, the spin  $I$  is addressed by the first chirp pulse, as given by

$$Eq.(S7) \xrightarrow{(\theta)_{\phi_c(t_I)}} e_1 \left[ \hat{I}^+ \cos^2 \frac{\theta}{2} + \hat{I}^- \sin^2 \frac{\theta}{2} \exp[i2\phi_c(t_I)] + \frac{i}{2} \sin \theta (\hat{I}_\alpha - \hat{I}_\beta) \exp[i\phi_c(t_I)] \right] \times \hat{S}_\alpha \exp \left[ -i(\Omega_I + \pi J_{IS}) \frac{t_1}{2} \right] \quad (S8)$$

With the aid of the gradient  $G_2$  and the CTP selection, only the zz terms  $(\hat{I}_\alpha - \hat{I}_\beta) \hat{S}_\alpha$  are reserved, and  $\pm 1$  order terms are removed, we have

$$Eq.(S8) \xrightarrow{\text{select zz terms}} \frac{i}{2} (\hat{I}_\alpha - \hat{I}_\beta) \hat{S}_\alpha e_1 \sin \theta \exp \left[ -i(\Omega_I + \pi J_{IS}) \frac{t_1}{2} \right] \exp[i\phi_c(t_I)] \quad (S9)$$

At the end of the  $t_S$  period, the spin  $S$  is addressed by the first chirp pulse, we have

$$\begin{aligned}
\text{Eq. (S9)} \xrightarrow{(\theta)_{\phi_c(t_S)}^S} & \frac{i}{2} (\hat{I}_\alpha - \hat{I}_\beta) \left\{ \hat{S}_\alpha \cos^2 \frac{\theta}{2} + \hat{S}_\beta \sin^2 \frac{\theta}{2} + \frac{i}{2} \hat{S}^+ \sin \theta \exp[-i\phi_c(t_S)] - \frac{i}{2} \hat{S}^- \sin \theta \exp[i\phi_c(t_S)] \right\} \\
& \times e_1 \sin \theta \exp \left[ -i(\Omega_I + \pi J_{IS}) \frac{t_1}{2} \right] \exp[i\phi_c(t_I)]
\end{aligned} \tag{S10}$$

Since the flip angle  $\theta$  is low, the intensity of  $\sin^2(\theta/2) \sin(\theta)$  is close to zero, the second term in the curly brace of Eq.(S10) is neglected. Furthermore, with the aid of the gradient  $G_2$  and the CTP selection, the  $\pm 1$  order terms in the curly brace of Eq.(S10) are removed. Hence, we have

$$\text{Eq. (S10)} \xrightarrow{\text{neglecting weak signals and CTP}} \frac{i}{2} (\hat{I}_\alpha - \hat{I}_\beta) \hat{S}_\alpha e_1 \sin \theta \cos^2 \frac{\theta}{2} \exp \left[ -i(\Omega_I + \pi J_{IS}) \frac{t_1}{2} \right] \exp[i\phi_c(t_I)] \tag{S11}$$

Eq. (S11) indicates that the term  $\hat{I}^+ \hat{S}_\alpha$  at the beginning of the first  $t_1/2$  is transferred to  $(\hat{I}_\alpha - \hat{I}_\beta) \hat{S}_\alpha$  by the first chirp pulse. The  $\alpha$  state of the passive spin  $S$  is not transferred to  $\beta$  state, vice versa. The  $zz$  terms  $(\hat{I}_\alpha - \hat{I}_\beta) \hat{S}_\alpha$  are kept unchanged until the second chirp pulse transfer these terms into observable terms. At the end of the  $t'_S$  period, the spin  $S$  is addressed by the second chirp pulse, as given by

$$\begin{aligned}
\text{Eq. (S11)} \xrightarrow{(\theta)_{\phi_{2c}(t'_S)}^S} & \frac{i}{2} (\hat{I}_\alpha - \hat{I}_\beta) \left\{ \hat{S}_\alpha \cos^2 \frac{\theta}{2} + \hat{S}_\beta \sin^2 \frac{\theta}{2} + \frac{i}{2} \hat{S}^+ \sin \theta \exp[-i\phi_{2c}(t'_S)] - \frac{i}{2} \hat{S}^- \sin \theta \exp[i\phi_{2c}(t'_S)] \right\} \\
& \times e_1 \sin \theta \cos^2 \frac{\theta}{2} \exp \left[ -i(\Omega_I + \pi J_{IS}) \frac{t_1}{2} \right] \exp[i\phi_c(t_I)]
\end{aligned} \tag{S12}$$

As the intensity of  $\sin^2(\theta/2) \sin(\theta)$  is close to zero, the second term in the curly brace of Eq. (S12) is neglected.

Furthermore, the  $\hat{S}^+$  related terms can't be observed in the acquisition period, we have

$$Eq.(S12) \xrightarrow{\text{neglecting weak signals and CTP}} \frac{i}{2} (\hat{I}_\alpha - \hat{I}_\beta) \left\{ \hat{S}_\alpha \cos^2 \frac{\theta}{2} - \frac{i}{2} \hat{S}^- \sin \theta \exp[i\phi_{2c}(t'_s)] \right\} \times e_1 \sin \theta \cos^2 \frac{\theta}{2} \exp \left[ -i(\Omega_I + \pi J_{IS}) \frac{t_1}{2} \right] \exp[i\phi_{1c}(t_I)] \quad (S13)$$

The single quantum terms  $(\hat{I}_\alpha - \hat{I}_\beta) \hat{S}^-$  in Eq. (S13) evolve during the  $t'_1 - t'_s$  period under the free precession Hamiltonian  $\hat{H}_{FP}$  and the gradient field  $G_2$ , we have

$$Eq.(S13) \xrightarrow{\hat{H}_{FP}(t'_1-t'_s) + \gamma G_2 z(t'_1-t'_s)} \frac{1}{4} \hat{I}_\alpha \hat{S}^- e_1 e_2 \sin^2 \theta \cos^2 \frac{\theta}{2} \exp \left[ -i(\Omega_I + \pi J_{IS}) \frac{t_1}{2} \right] \exp[i\phi_{1c}(t_I) + i\phi_{2c}(t'_s)] - \frac{1}{4} \hat{I}_\beta \hat{S}^- e_1 e_3 \sin^2 \theta \cos^2 \frac{\theta}{2} \exp \left[ -i(\Omega_I + \pi J_{IS}) \frac{t_1}{2} \right] \exp[i\phi_{1c}(t_I) + i\phi_{2c}(t'_s)] + \frac{i}{2} (\hat{I}_\alpha - \hat{I}_\beta) \hat{S}_\alpha e_1 \sin \theta \cos^4 \frac{\theta}{2} \exp \left[ -i(\Omega_I + \pi J_{IS}) \frac{t_1}{2} \right] \exp[i\phi_{1c}(t_I)] \quad (S14)$$

where

$$e_2 = \exp \left[ i(\Omega_S + \pi J_{IS})(t'_1 - t'_s) + i\gamma G_2 z(t'_1 - t'_s) \right] e_3 = \exp \left[ i(\Omega_S - \pi J_{IS})(t'_1 - t'_s) + i\gamma G_2 z(t'_1 - t'_s) \right] \quad (S15)$$

At the end of the  $t'_1$  period, the spin  $I$  is addressed by the second chirp pulse, as given by

Eq.(S14)  $\xrightarrow{(\theta)_{\phi_{2c}(t')}} \rightarrow$

$$\begin{aligned}
& \frac{1}{4} \left\{ \hat{I}_\alpha \cos^2 \frac{\theta}{2} + \hat{I}_\beta \sin^2 \frac{\theta}{2} + \frac{i}{2} \hat{I}^+ \sin \theta \exp[-i\phi_{2c}(t')] - \frac{i}{2} \hat{I}^- \sin \theta \exp[i\phi_{2c}(t')] \right\} \hat{S}^- \\
& \quad \times e_1 e_2 \sin^2 \theta \cos^2 \frac{\theta}{2} \exp \left[ -i(\Omega_I + \pi J_{IS}) \frac{t_1}{2} \right] \exp[i\phi_{1c}(t) + i\phi_{2c}(t')] \\
& - \frac{1}{4} \left\{ \hat{I}_\beta \cos^2 \frac{\theta}{2} + \hat{I}_\alpha \sin^2 \frac{\theta}{2} - \frac{i}{2} \hat{I}^+ \sin \theta \exp[-i\phi_{2c}(t')] + \frac{i}{2} \hat{I}^- \sin \theta \exp[i\phi_{2c}(t')] \right\} \hat{S}^- \\
& \quad \times e_1 e_3 \sin^2 \theta \cos^2 \frac{\theta}{2} \exp \left[ -i(\Omega_I + \pi J_{IS}) \frac{t_1}{2} \right] \exp[i\phi_{1c}(t) + i\phi_{2c}(t')] \\
& + \frac{i}{2} \left\{ \hat{I}_\alpha \cos^2 \frac{\theta}{2} + \hat{I}_\beta \sin^2 \frac{\theta}{2} + \frac{i}{2} \hat{I}^+ \sin \theta \exp[-i\phi_{2c}(t')] - \frac{i}{2} \hat{I}^- \sin \theta \exp[i\phi_{2c}(t')] \right\} \hat{S}_\alpha \\
& \quad \times e_1 \sin \theta \cos^4 \frac{\theta}{2} \exp \left[ -i(\Omega_I + \pi J_{IS}) \frac{t_1}{2} \right] \exp[i\phi_{1c}(t)] \\
& - \frac{i}{2} \left\{ \hat{I}_\beta \cos^2 \frac{\theta}{2} + \hat{I}_\alpha \sin^2 \frac{\theta}{2} - \frac{i}{2} \hat{I}^+ \sin \theta \exp[-i\phi_{2c}(t')] + \frac{i}{2} \hat{I}^- \sin \theta \exp[i\phi_{2c}(t')] \right\} \hat{S}_\alpha \\
& \quad \times e_1 \sin \theta \cos^4 \frac{\theta}{2} \exp \left[ -i(\Omega_I + \pi J_{IS}) \frac{t_1}{2} \right] \exp[i\phi_{1c}(t)]
\end{aligned} \tag{S16}$$

As the intensity of  $\sin^2(\theta/2) \sin(\theta)$  is close zero, and the unobservable terms in Eq.(S16) are neglected, we have

Eq.(S16)  $\xrightarrow{\text{neglecting weak signals and CTP}} \rightarrow$

$$\begin{aligned}
& \frac{1}{4} \hat{I}_\alpha \hat{S}^- e_1 e_2 \sin^2 \theta \cos^4 \frac{\theta}{2} \exp \left[ -i(\Omega_I + \pi J_{IS}) \frac{t_1}{2} \right] \exp[i\phi_{1c}(t) + i\phi_{2c}(t')] \\
& - \frac{1}{4} \hat{I}_\beta \hat{S}^- e_1 e_3 \sin^2 \theta \cos^4 \frac{\theta}{2} \exp \left[ -i(\Omega_I + \pi J_{IS}) \frac{t_1}{2} \right] \exp[i\phi_{1c}(t) + i\phi_{2c}(t')] \\
& + \frac{1}{2} \hat{I}^- \hat{S}_\alpha e_1 \sin^2 \theta \cos^4 \frac{\theta}{2} \exp \left[ -i(\Omega_I + \pi J_{IS}) \frac{t_1}{2} \right] \exp[i\phi_{1c}(t) + i\phi_{1c}(t')]
\end{aligned} \tag{S17}$$

All terms in Eq. (S17) can be obtained during the acquisition period. Considering these terms evolve under the free precession Hamiltonian  $\hat{H}_{FP}$  and the gradient fields  $G_1$  and  $G_2$  before acquisition, we have



Eq.(S17)  $\xrightarrow{\hat{H}_{FP}(t_1+\delta_1+\frac{t_1+t_2}{2})+\gamma G_2 z t_1+\gamma G_2 z \delta_1}$

$$\begin{aligned} & \frac{1}{4} \hat{I}_\alpha \hat{S}^- e_1 e_2 e_4 \sin^2 \theta \cos^4 \frac{\theta}{2} \exp \left[ -i(\Omega_I - \Omega_S) \frac{t_1}{2} \right] \exp \left[ i(\Omega_S + \pi J_{IS}) t_2 \right] \exp \left[ i\phi_{1c}(t_1) + i\phi_{2c}(t'_S) \right] \\ & - \frac{1}{4} \hat{I}_\beta \hat{S}^- e_1 e_3 e_5 \sin^2 \theta \cos^4 \frac{\theta}{2} \exp \left[ -i(\Omega_I - \Omega_S + \pi 2J_{IS}) \frac{t_1}{2} \right] \exp \left[ i(\Omega_S - \pi J_{IS}) t_2 \right] \exp \left[ i\phi_{1c}(t_1) + i\phi_{2c}(t'_S) \right] \\ & + \frac{1}{2} \hat{I}^- \hat{S}^- e_1 e_6 \sin^2 \theta \cos^4 \frac{\theta}{2} \exp \left[ i(\Omega_I + \pi J_{IS}) t_2 \right] \exp \left[ i\phi_{1c}(t_1) + i\phi_{1c}(t'_I) \right] \end{aligned}$$

(S18)

where

$$\begin{aligned} e_4 &= \exp \left[ i(\Omega_S + \pi J_{IS})(t_1 + \delta_1) + i\gamma G_2 z t_1 + i\gamma G_1 z \delta_1 \right] \\ e_5 &= \exp \left[ i(\Omega_S - \pi J_{IS})(t_1 + \delta_1) + i\gamma G_2 z t_1 + i\gamma G_1 z \delta_1 \right] \\ e_6 &= \exp \left[ i(\Omega_I + \pi J_{IS})(t_1 + \delta_1) + i\gamma G_2 z t_1 + i\gamma G_1 z \delta_1 \right] \end{aligned}$$

(S19)

Substituting in  $t_{I/S}, t'_{I/S}$  in Eq. (S5),  $e_1$  in Eq. (S7),  $e_2, e_3$  in Eq. (S15),  $e_4, e_5, e_6$  in Eq.(S19),  $\phi_{1c}(t_1)$ ,

$\phi_{2c}(t'_S)$  and  $\phi_{2c}(t'_I)$  in Eq. (S5) gives

$$\begin{aligned} e_1 e_2 e_4 \exp \left[ i\phi_{1c}(t_1) + i\phi_{2c}(t'_S) \right] &= e_7 \exp \left[ i \frac{(\Omega_S - \Omega_I) \gamma G_2 z}{R} \right] \\ e_1 e_3 e_5 \exp \left[ i\phi_{1c}(t_1) + i\phi_{2c}(t'_S) \right] &= e_8 \exp \left[ -i \frac{(\Omega_S - \Omega_I - 2\pi J_{IS}) \gamma G_2 z}{R} \right] \\ e_1 e_6 \exp \left[ i\phi_{1c}(t_1) + i\phi_{2c}(t'_I) \right] &= 1. \end{aligned}$$

(S20)

where

$$\begin{aligned} e_7 &= \exp \left[ i(\Omega_S - \Omega_I) \left( -\frac{\Omega_I}{R} + \frac{O_i}{R} + \delta_1 \right) \right] \exp \left[ i(\Omega_S + \pi J_{IS}) \left( \frac{\Omega_S - \Omega_I}{R} \right) \right] \exp \left[ i \frac{(\Omega_S^2 - \Omega_I^2)}{2R} \right] \\ e_8 &= \exp \left[ i(\Omega_S - \Omega_I - 2\pi J_{IS}) \left( -\frac{\Omega_I}{R} + \frac{O_i}{R} + \delta_1 \right) \right] \exp \left[ i(\Omega_S - \pi J_{IS}) \left( \frac{\Omega_S - \Omega_I}{R} \right) \right] \exp \left[ i \frac{(\Omega_S^2 - \Omega_I^2)}{2R} \right] \end{aligned}$$

(S21)

Substituting Eq. (S20) and Eq. (S21) in Eq. (S18), we have

$$\begin{aligned}
A_\alpha(t_1, t_2, z) = & \\
& \frac{1}{4} c \left\{ \begin{aligned} & \hat{I}_\alpha \hat{S}^- e_7 \exp \left[ i(\Omega_S - \Omega_I) \frac{t_1}{2} \right] \exp \left[ i(\Omega_S + \pi J_{IS}) t_2 \right] \exp \left[ i \frac{(\Omega_S - \Omega_I) \gamma G_2 z}{R} \right] \\ & - \hat{I}_\beta \hat{S}^- e_8 \exp \left[ i(\Omega_S - \Omega_I - 2\pi J_{IS}) \frac{t_1}{2} \right] \exp \left[ i(\Omega_S - \pi J_{IS}) t_2 \right] \exp \left[ -i \frac{(\Omega_S - \Omega_I - 2\pi J_{IS}) \gamma G_2 z}{R} \right] \end{aligned} \right\} \quad (S22) \\
& + \frac{1}{2} \hat{I}^- \hat{S}_\alpha c \exp \left[ i(\Omega_I + \pi J_{IS}) t_2 \right]
\end{aligned}$$

where  $c = \sin^2 \theta \cos^4 \frac{\theta}{2}$ .

Eq. (S22) demonstrates that the first two terms correspond to cross-peaks since the coherence term of  $\hat{I}^+ \hat{S}_\alpha$  at the beginning of the first  $t_1/2$  period is transferred to  $\hat{I}_\alpha \hat{S}^-$  and  $\hat{I}_\beta \hat{S}^-$ . The third term corresponds to axial-peak since the coherence term  $\hat{I}^+ \hat{S}_\alpha$  is transferred to  $\hat{I}^- \hat{S}_\alpha$ . It is needed to observed that the first two terms in Eq. (S22) are modulated by the phase  $2(\Omega_S - \Omega_I) \gamma G_2 z / R$ , which is linearly dependent on the  $z$  axis. When averaging over the effective sample height  $h$ , we can obtain the total signal as follows:

$$\begin{aligned}
A_\alpha(t_1, t_2) = & \\
& \frac{c}{4} \left\{ \begin{aligned} & \hat{I}_\alpha \hat{S}^- e_7 \exp \left[ i(\Omega_S - \Omega_I) \frac{t_1}{2} \right] \exp \left[ i(\Omega_S + \pi J_{IS}) t_2 \right] \text{sinc} \left[ \frac{(\Omega_S - \Omega_I) \gamma G_2 h}{2R} \right] \\ & - \hat{I}_\beta \hat{S}^- e_8 \exp \left[ i(\Omega_S - \Omega_I - 2\pi J_{IS}) \frac{t_1}{2} \right] \exp \left[ i(\Omega_S - \pi J_{IS}) t_2 \right] \text{sinc} \left[ \frac{(\Omega_S - \Omega_I - 2\pi J_{IS}) \gamma G_2 h}{2R} \right] \end{aligned} \right\} \quad (S23) \\
& + \frac{1}{2} \hat{I}^- \hat{S}_\alpha c \exp \left[ i(\Omega_I + \pi J_{IS}) t_2 \right]
\end{aligned}$$

Similarly, the above derivation is applicable for the single quantum term  $\hat{I}^+ \hat{S}_\beta$  in Eq. (S1), we have

$$\begin{aligned}
A_\beta(t_1, t_2) = & \\
& \frac{c}{4} \left\{ \begin{aligned} & -\hat{I}_\alpha \hat{S}^- e_9 c \exp \left[ i(\Omega_S - \Omega_I + 2\pi J_{IS}) \frac{t_1}{2} \right] \exp \left[ i(\Omega_S + \pi J_{IS}) t_2 \right] \operatorname{sinc} \left[ \frac{(\Omega_S - \Omega_I + 2\pi J_{IS}) \gamma G_2 h}{2R} \right] \\ & + \hat{I}_\beta \hat{S}^- e_{10} c \exp \left[ i(\Omega_S - \Omega_I) \frac{t_1}{2} \right] \exp \left[ i(\Omega_S - \pi J_{IS}) t_2 \right] \operatorname{sinc} \left[ \frac{(\Omega_S - \Omega_I) \gamma G_2 h}{2R} \right] \end{aligned} \right\} \quad (\text{S24}) \\
& + \frac{1}{2} \hat{I}^- \hat{S}_\beta c \exp \left[ i(\Omega_I - \pi J_{IS}) t_2 \right]
\end{aligned}$$

where

$$\begin{aligned}
e_9 = & \exp \left[ i(\Omega_S - \Omega_I + 2\pi J_{IS}) \left( -\frac{\Omega_I}{R} + \frac{O_i}{R} + \delta_1 \right) \right] \exp \left[ i(\Omega_S + \pi J_{IS}) \frac{(\Omega_S - \Omega_I)}{R} \right] \exp \left[ i \frac{(\Omega_S^2 - \Omega_I^2)}{2R} \right] \\
e_{10} = & \exp \left[ i(\Omega_S - \Omega_I) \left( -\frac{\Omega_I}{R} + \frac{O_i}{R} + \delta_1 \right) \right] \exp \left[ i(\Omega_S - \pi J_{IS}) \frac{(\Omega_S - \Omega_I)}{R} \right] \exp \left[ i \frac{(\Omega_S^2 - \Omega_I^2)}{2R} \right]
\end{aligned} \quad (\text{S25})$$

If we combine Eq. (S23) with Eq.(S24), the signals of cross peaks and axial peaks originated from  $\hat{I}^+ \hat{S}_\alpha$  and  $\hat{I}^+ \hat{S}_\beta$  are obtained,

$$\begin{aligned}
A(t_1, t_2) = & \\
& \frac{c}{4} \left\{ \begin{aligned} & \hat{I}_\alpha \hat{S}^- e_7 \exp \left[ i(\Omega_S - \Omega_I) \frac{t_1}{2} \right] \exp \left[ i(\Omega_S + \pi J_{IS}) t_2 \right] \operatorname{sinc} \left[ \frac{(\Omega_S - \Omega_I) \gamma G_2 h}{2R} \right] \\ & - \hat{I}_\beta \hat{S}^- e_8 \exp \left[ i(\Omega_S - \Omega_I - 2\pi J_{IS}) \frac{t_1}{2} \right] \exp \left[ i(\Omega_S - \pi J_{IS}) t_2 \right] \operatorname{sinc} \left[ \frac{(\Omega_S - \Omega_I - 2\pi J_{IS}) \gamma G_2 h}{2R} \right] \\ & - \hat{I}_\alpha \hat{S}^- e_9 \exp \left[ i(\Omega_S - \Omega_I + 2\pi J_{IS}) \frac{t_1}{2} \right] \exp \left[ i(\Omega_S + \pi J_{IS}) t_2 \right] \operatorname{sinc} \left[ \frac{(\Omega_S - \Omega_I + 2\pi J_{IS}) \gamma G_2 h}{2R} \right] \\ & + \hat{I}_\beta \hat{S}^- e_{10} \exp \left[ i(\Omega_S - \Omega_I) \frac{t_1}{2} \right] \exp \left[ i(\Omega_S - \pi J_{IS}) t_2 \right] \operatorname{sinc} \left[ \frac{(\Omega_S - \Omega_I) \gamma G_2 h}{2R} \right] \end{aligned} \right\} \quad (\text{S26}) \\
& + \frac{c}{2} \hat{I}^- \hat{S}_\alpha \exp \left[ i(\Omega_I + \pi J_{IS}) t_2 \right] + \frac{c}{2} \hat{I}^- \hat{S}_\beta \exp \left[ i(\Omega_I - \pi J_{IS}) t_2 \right]
\end{aligned}$$

When the derivation is from either  $\hat{S}^+ \hat{I}_\alpha$  or  $\hat{S}^+ \hat{I}_\beta$ , we have the similar formula in the end.

The above derivation demonstrates that for the two-spin system  $IS$ , the CTP of the cross peaks is:

$$\hat{I}^+ \hat{S}_\alpha \rightarrow (\hat{I}_\alpha - \hat{I}_\beta) \hat{S}_\alpha \rightarrow (\hat{I}_\alpha - \hat{I}_\beta) \hat{S}^-, \text{ and the CTP of the axis peak is } \hat{I}^+ \hat{S}_\alpha \rightarrow (\hat{I}_\alpha - \hat{I}_\beta) \hat{S}_\alpha \rightarrow \hat{I}^- \hat{S}_\alpha.$$

In both CTPs, the term  $\hat{I}^+ \hat{S}_\alpha$  is transferred to  $(\hat{I}_\alpha - \hat{I}_\beta) \hat{S}_\alpha$  by the first chirp pulse with a low flip angle. It is needed to note that the  $\alpha$  state of the passive spin  $S$  is not transferred to  $\beta$  state by the chirp pulse. Similarly, the  $\beta$  state of the passive spin  $S$  is not transferred to  $\alpha$  state by the chirp pulse. When extending to the three-spin system  $ISS'$ , where  $S'$  represents another passive spin, and the CTP corresponding to cross-peaks is either  $\hat{I}^+ \hat{S}_\alpha \hat{S}'_\alpha \rightarrow (\hat{I}_\alpha - \hat{I}_\beta) \hat{S}_\alpha \hat{S}'_\alpha \rightarrow (\hat{I}_\alpha - \hat{I}_\beta) \hat{S}'_\alpha \hat{S}^-$  or  $\hat{I}^+ \hat{S}_\alpha \hat{S}'_\beta \rightarrow (\hat{I}_\alpha - \hat{I}_\beta) \hat{S}_\alpha \hat{S}'_\beta \rightarrow (\hat{I}_\alpha - \hat{I}_\beta) \hat{S}'_\beta \hat{S}^-$ , and the CTP corresponding to axial peaks is either  $\hat{I}^+ \hat{S}_\alpha \hat{S}'_\alpha \rightarrow (\hat{I}_\alpha - \hat{I}_\beta) \hat{S}_\alpha \hat{S}'_\alpha \rightarrow \hat{I}^- \hat{S}_\alpha \hat{S}'_\alpha$  or  $\hat{I}^+ \hat{S}_\alpha \hat{S}'_\beta \rightarrow (\hat{I}_\alpha - \hat{I}_\beta) \hat{S}_\alpha \hat{S}'_\beta \rightarrow \hat{I}^- \hat{S}_\alpha \hat{S}'_\beta$ . Compared with the two-spin system  $IS$ , a replication of basic multiplets is observed in the three-spin system  $ISS'$ , as shown in Fig. 2(b and c). In the case of three-spin systems, the pattern of multiplets in 2D CHEESE spectra is similar to that in E. COSY spectra, basic multiplets are replicated once as shown in Fig.2. As for the three-spin system in COSY spectra, due to the  $\alpha$  state of passive spins is transferred to  $\beta$  state in the mixing time, vice versa, basic multiplets of the two-spin system are replicated three times. Therefore, as for higher multi-spin systems, the multiplets in COSY spectra are increased more than those in CHEESE spectra.

For the case of two-spin strongly coupled  $IS$  systems, where  $|\Omega_I - \Omega_S| \leq 6|J_{IS}|$ , the formalism of free precession Hamiltonian  $\hat{H}'_{FP}$  should be as follow:

$$\hat{H}'_{FP} = \Omega_I \hat{I}_z + \Omega_S \hat{S}_z + \pi J_{IS} 2(\hat{I}_x \hat{S}_x + \hat{I}_y \hat{S}_y + \hat{I}_z \hat{S}_z) \quad (\text{S27})$$

The product basis functions and energy in weakly coupled systems are no longer those of strongly coupled systems. The eigenfunctions and eigenvalues of  $\hat{H}'_{FP}$  is

<i>Energy</i>	<i>Basis function</i>
$E'_1 = \frac{1}{2}(\Omega_I + \Omega_S + \pi J_{IS})$	$ \alpha\alpha\rangle$
$E'_2 = \frac{1}{2}(\Delta\Omega - \pi J_{IS})$	$\cos(\lambda) \alpha\beta\rangle - \sin(\lambda) \beta\alpha\rangle$
$E'_3 = \frac{1}{2}(-\Delta\Omega - \pi J_{IS})$	$\cos(\lambda) \beta\alpha\rangle + \sin(\lambda) \alpha\beta\rangle$
$E'_4 = \frac{1}{2}(-\Omega_I - \Omega_S + \pi J_{IS})$	$ \beta\beta\rangle$

where the parameters  $\lambda$  and  $\Delta\Omega$  are defined as  $\tan(2\lambda) = \frac{2\pi J_{IS}}{\Omega_I - \Omega_S}$ ,  $\Delta\Omega = \sqrt{(\Omega_I - \Omega_S)^2 + (2\pi J_{IS})^2}$ .

According to the representation of ref. [2], the new set of single-element basis operators with the use of curly braces can be used to represent the 16 elements of  $\hat{\rho}_{ij}$  in the new basis functions. For example,  $\{\hat{I}^+ \hat{S}_\alpha\}$  represents  $\hat{\rho}_{13}$  when  $\hat{\rho}$  is written in the strongly coupled basis. The evolution of the coherence term  $\{\hat{I}^+ \hat{S}_\alpha\}$  is presented as

$$\{\hat{I}^+ \hat{S}_\alpha\} \xrightarrow{\hat{H}_{FP} \frac{t_1}{2}} \{\hat{I}^+ \hat{S}_\alpha\} \exp\left[i(E'_3 - E'_1) \frac{t_1}{2}\right] \quad (\text{S28})$$

When the term  $\{\hat{I}^+ \hat{S}_\alpha\}$  is observed in the original basis function, we have

$$\{\hat{I}^+ \hat{S}_\alpha\} = \cos(\lambda) \hat{I}^+ \hat{S}_\alpha + \sin(\lambda) \hat{I}_\alpha \hat{S}^+ \quad (\text{S29})$$

According to the derivation from Eq. (S8) to Eq. (S23), we have

$$\begin{aligned}
& \hat{I}^+ \hat{S}_\alpha \xrightarrow{(\theta)_{\hat{a}_c(t)}^I} \xrightarrow{(\theta)_{\hat{a}_c(t_S)}^S} \xrightarrow{(\theta)_{\hat{a}_c(t_S)}^S} \xrightarrow{\hat{H}_{FP}(t'_I - t'_S) + \gamma G_2 z(t'_I - t'_S)} \xrightarrow{(\theta)_{\hat{a}_c(t)}^I} \\
& \frac{c}{4} \left\{ \begin{array}{l} \hat{I}_\alpha \hat{S}^- e_{11} \exp \left[ i \frac{\Delta \Omega \gamma G_2 z}{R} \right] \\ - \hat{I}_\beta \hat{S}^- e_{12} \exp \left[ i \frac{(\Delta \Omega + 2\pi J_{IS}) \gamma G_2 z}{R} \right] \end{array} \right\} + \frac{c}{2} \hat{I}^- \hat{S}_\alpha \\
& \hat{I}_\alpha \hat{S}^+ \xrightarrow{(\theta)_{\hat{a}_c(t)}^I} \xrightarrow{(\theta)_{\hat{a}_c(t_S)}^S} \xrightarrow{(\theta)_{\hat{a}_c(t_S)}^S} \xrightarrow{\hat{H}_{FP}(t'_I - t'_S) + \gamma G_2 z(t'_I - t'_S)} \xrightarrow{(\theta)_{\hat{a}_c(t)}^I}
\end{aligned} \tag{S30}$$

$$\frac{c}{4} \left\{ \begin{array}{l} \hat{I}^- \hat{S}_\alpha e_{13} \exp \left[ -i \frac{\Delta \Omega \gamma G_2 z}{R} \right] \\ - \hat{I}^- \hat{S}_\beta e_{14} \exp \left[ -i \frac{(\Delta \Omega - 2\pi J_{IS}) \gamma G_2 z}{R} \right] \end{array} \right\} + \frac{c}{2} \hat{I}_\alpha \hat{S}^-$$

where,

$$\begin{aligned}
e_{11} &= \exp \left[ i \Delta \Omega \left( \frac{-\Omega_I + O_i}{R} + \delta_1 \right) \right] \exp \left[ i \{ \Omega_S + \pi J_{IS} \} \left( \frac{\Omega_I - \Omega_S}{R} \right) \right] \exp \left[ i \frac{\Omega_S^2 - \Omega_I^2}{2R} \right] \\
e_{12} &= \exp \left[ i \{ \Delta \Omega + 2\pi J_{IS} \} \left( \frac{-\Omega_I + O_i}{R} + \delta_1 \right) \right] \exp \left[ i \{ \Omega_S - \pi J_{IS} \} \left( \frac{\Omega_I - \Omega_S}{R} \right) \right] \exp \left[ i \frac{\Omega_S^2 - \Omega_I^2}{2R} \right] \\
e_{13} &= \exp \left\{ i \left[ \{ \Omega_S + \pi J_{IS} \} \frac{\Omega_S}{R} - \{ \Omega_I + \pi J_{IS} \} \frac{\Omega_I}{R} \right] \right\} \exp \left\{ i \Delta \Omega \left( \frac{O_i}{R} + \delta_1 \right) \right\} \exp \left[ \frac{\Omega_I^2 - \Omega_S^2}{2R} \right] \\
e_{14} &= \exp \left\{ i \left[ \{ \Omega_S + \pi J_{IS} \} \frac{\Omega_S}{R} - \{ \Omega_I - \pi J_{IS} \} \frac{\Omega_I}{R} \right] \right\} \exp \left\{ i \{ \Delta \Omega - 2\pi J_{IS} \} \left( \frac{O_i}{R} + \delta_1 \right) \right\} \exp \left[ \frac{\Omega_I^2 - \Omega_S^2}{2R} \right]
\end{aligned} \tag{S31}$$

where

$$\begin{aligned}
\{ \Omega_S + \pi J_{IS} \} &\equiv \frac{1}{2} (\Omega_I + \Omega_S - \Delta \Omega) + \pi J_{IS} \\
\{ \Omega_S - \pi J_{IS} \} &\equiv \frac{1}{2} (\Omega_I + \Omega_S - \Delta \Omega) - \pi J_{IS} \\
\{ \Omega_I + \pi J_{IS} \} &\equiv \frac{1}{2} (\Omega_I + \Omega_S + \Delta \Omega) + \pi J_{IS} \\
\{ \Omega_I - \pi J_{IS} \} &\equiv \frac{1}{2} (\Omega_I + \Omega_S + \Delta \Omega) - \pi J_{IS}
\end{aligned} \tag{S32}$$

When the single-element basis operators are observed in the new basis function, we have

$$\begin{aligned}
I^-S_\alpha &= \cos(\lambda) \{I^-S_\alpha\} - \sin(\lambda) \{I_\alpha S^-\} \\
I_\alpha S^- &= \sin(\lambda) \{I^-S_\alpha\} + \cos(\lambda) \{I_\alpha S^-\} \\
I^-S_\beta &= \cos(\lambda) \{I^-S_\beta\} + \sin(\lambda) \{I_\beta S^-\} \\
I_\beta S^- &= \cos(\lambda) \{I_\beta S^-\} - \sin(\lambda) \{I^-S_\beta\}
\end{aligned} \tag{S33}$$

Substituting (S33) into (S30), we have

$$\begin{aligned}
(S.29) &= \{\hat{I}^+ \hat{S}_\alpha\} \xrightarrow{\text{chirp pulses}} \\
&\left. \begin{aligned}
&\left\{ \{I_\alpha S^-\} \left[ c_1 e_{11} \exp\left(i \frac{\Delta\Omega \gamma G_2 z}{R}\right) - s_1 e_{13} \exp\left(-i \frac{\Delta\Omega \gamma G_2 z}{R}\right) \right] \right. \\
&- \left. \{I_\beta S^-\} \left\{ c_1 e_{12} \exp\left[i \frac{(\Delta\Omega + 2\pi J_{IS}) \gamma G_2 z}{R}\right] - s_1 e_{14} \exp\left[-i \frac{(\Delta\Omega - 2\pi J_{IS}) \gamma G_2 z}{R}\right] \right\} \right\} \\
&+ \left\{ I^-S_\alpha \right\} \left[ 2 + c_2 e_{11} \exp\left(i \frac{\Delta\Omega \gamma G_2 z}{R}\right) + c_2 e_{13} \exp\left(-i \frac{\Delta\Omega \gamma G_2 z}{R}\right) \right] \\
&+ \left. \left\{ I^-S_\beta \right\} \left\{ c_2 e_{12} \exp\left[i \frac{(\Delta\Omega + 2\pi J_{IS}) \gamma G_2 z}{R}\right] - c_2 e_{14} \exp\left[-i \frac{(\Delta\Omega - 2\pi J_{IS}) \gamma G_2 z}{R}\right] \right\} \right\}
\end{aligned} \right\} \frac{c}{4} \tag{S34}
\end{aligned}$$

where  $c_1 = \cos^2(\lambda)$ ,  $s_1 = \sin^2(\lambda)$ ,  $c_2 = \cos(\lambda)\sin(\lambda)$ .

When considering evolution during the  $t_1$  and  $t_2$  periods, we have

$$\begin{aligned}
(S.29) &= \{\hat{I}^+ \hat{S}_\alpha\} \xrightarrow{\hat{H}'_{FP} \frac{t_1}{2}} \xrightarrow{\text{chirp pulses}} \xrightarrow{\hat{H}'_{FP} \frac{t_1}{2}} \xrightarrow{\hat{H}'_{FP} t_2} \\
&\left\{ \begin{aligned}
&\left\{ I_\alpha^- S^- \right\} \exp\left(-i\Delta\Omega \frac{t_1}{2}\right) \exp\left(i\{\Omega_S + \pi J_{IS}\}t_2\right) \begin{bmatrix} c_1 e_{11} \exp\left(i\frac{\Delta\Omega\gamma G_2 z}{R}\right) \\ -s_1 e_{13} \exp\left(-i\frac{\Delta\Omega\gamma G_2 z}{R}\right) \end{bmatrix} \\
&- \left\{ I_\beta^- S^- \right\} \exp\left[-i(\Delta\Omega + 2\pi J_{IS})\frac{t_1}{2}\right] \exp\left(i\{\Omega_S - \pi J_{IS}\}t_2\right) \begin{bmatrix} c_1 e_{12} \exp\left[i\frac{(\Delta\Omega + 2\pi J_{IS})\gamma G_2 z}{R}\right] \\ -s_1 e_{14} \exp\left[-i\frac{(\Delta\Omega - 2\pi J_{IS})\gamma G_2 z}{R}\right] \end{bmatrix} \\
&+ \left\{ I^- S_\alpha \right\} \exp\left(i\{\Omega_I + \pi J_{IS}\}t_2\right) \left\{ 2 + c_2 e_{11} \exp\left(i\frac{\Delta\Omega\gamma G_2 z}{R}\right) + c_2 e_{13} \exp\left(-i\frac{\Delta\Omega\gamma G_2 z}{R}\right) \right\} \\
&+ \left\{ I^- S_\beta \right\} \exp\left(i\{-\pi J_{IS}\}t_1\right) \exp\left(i\{\Omega_I - \pi J_{IS}\}t_2\right) \begin{bmatrix} c_2 e_{12} \exp\left[i\frac{(\Delta\Omega + 2\pi J_{IS})\gamma G_2 z}{R}\right] \\ -c_2 e_{14} \exp\left[-i\frac{(\Delta\Omega - 2\pi J_{IS})\gamma G_2 z}{R}\right] \end{bmatrix}
\end{aligned} \right\} \frac{c}{4}
\end{aligned} \tag{S35}$$

When averaging over the effective sample height  $h$ , we can obtain the signal as follows:

$$\begin{aligned}
A_{\alpha\text{-strong}}(t_1, t_2) &= \\
&\left\{ \begin{aligned}
&\left\{ I_\alpha^- S^- \right\} \exp\left(-i\Delta\Omega \frac{t_1}{2}\right) \exp\left(i\{\Omega_S + \pi J_{IS}\}t_2\right) (c_1 e_{11} - s_1 e_{13}) \text{sinc}\left(\frac{\Delta\Omega\gamma G_2 z}{2R}\right) \\
&- \left\{ I_\beta^- S^- \right\} \exp\left[-i(\Delta\Omega + 2\pi J_{IS})\frac{t_1}{2}\right] \exp\left(i\{\Omega_S - \pi J_{IS}\}t_2\right) \begin{bmatrix} c_1 e_{12} \text{sinc}\left[\frac{(\Delta\Omega + 2\pi J_{IS})\gamma G_2 z}{2R}\right] \\ -s_1 e_{14} \text{sinc}\left[\frac{(\Delta\Omega - 2\pi J_{IS})\gamma G_2 z}{2R}\right] \end{bmatrix} \\
&+ \left\{ I^- S_\alpha \right\} \exp\left(i\{\Omega_I + \pi J_{IS}\}t_2\right) \left[ 2 + c_2 (e_{11} + e_{13}) \text{sinc}\left(\frac{\Delta\Omega\gamma G_2 z}{2R}\right) \right] \\
&+ \left\{ I^- S_\beta \right\} \exp\left(i\{-\pi J_{IS}\}t_1\right) \exp\left(i\{\Omega_I - \pi J_{IS}\}t_2\right) \begin{bmatrix} c_2 e_{12} \text{sinc}\left[\frac{(\Delta\Omega + 2\pi J_{IS})\gamma G_2 z}{2R}\right] \\ -c_2 e_{14} \text{sinc}\left[\frac{(\Delta\Omega - 2\pi J_{IS})\gamma G_2 z}{2R}\right] \end{bmatrix}
\end{aligned} \right\} \frac{c}{4}
\end{aligned} \tag{S36}$$



The first two terms in Eq. (S36) are corresponding to cross peaks, and the last two terms corresponding to axial peaks. Compared Eq. (S23) with Eq. (S36), it is observed that an extra axis peak arising from  $\{\hat{I}^-\hat{S}_\beta\}$  in the fourth term arise, the intensity of cross peaks arising from  $\{\hat{I}_\alpha\hat{S}^-\}$  and  $\{\hat{I}_\beta\hat{S}^-\}$ , and the intensity of the axis peak arising from  $\{\hat{I}^-\hat{S}_\alpha\}$  are varied.

## 2. Experimental details

All experiments were performed on a 500 MHz Varian NMR spectrometer equipped with a 5 mm  $^1\text{H}$  XYZ indirect detection probe with 3D gradient coils. The duration of the non-selective  $90^\circ$  pulse was 8.55  $\mu\text{s}$ . Each chirp pulse was set with a duration of 15 ms, sweep width of 10 kHz, and flip angle  $\theta$  of  $15^\circ$  in all CHEESE experiments. The coherence selection gradients  $G_1$  were set with amplitudes of 10.51 G/cm and durations of 1.0 ms. The weak gradient  $G_2$  matching with chirp pulses was centered at the pulse element of two chirp pulses with its amplitude of 0.74 G/cm. The pulse repetition time was 2.0 s.

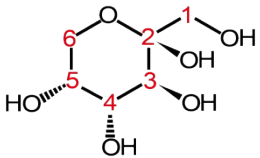
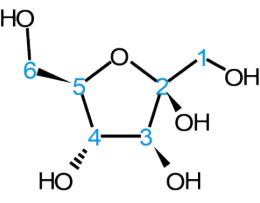
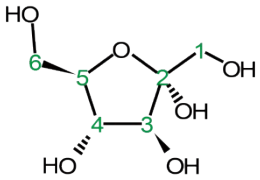
As for the experiment of performing the E. COSY sequence on the solution of inosine and quinine in DMSO- $d_6$ , the spectral bandwidths of  $SW$  and  $SW_1$  in both dimensions were set to 5 kHz. The number of  $t_1$  increments was set to 1024. Four-step phase cycling was applied. The pulse repetition time was 1.0 s. The experiment time was 2 h 51 min.

As for the experiment of performing the CHEESE sequence on the solution of inosine and quinine in DMSO- $d_6$ , the spectral bandwidths of  $SW_1$  in the  $F_1$  dimension was set to 100 Hz, the number of  $t_1$  increments were set to 128. Four-step phase cycling was applied, and the experiment time was 1 h 2 min.

As for the experiment of performing the CHEESE sequence on the solution of D-fructose in  $\text{D}_2\text{O}$ , the spectral bandwidths of  $SW_1$  in the  $F_1$  dimension were set to 200 Hz, the number of  $t_1$  increments were set to 512. Eight-step phase cycling was applied, and the experiment time was 4 h 56 min.

### 3. Chemical shifts and $J$ -coupling constants of coupled protons in D-fructose

**Table S1 Chemical shifts and  $J$ -coupling constants of three main tautomers in D-fructose**

Molecule	Position	Chemical shift (ppm)			$J$ -coupling (Hz)
		Previous work*	Our work	Difference	
 <p><b><math>\beta</math>-pyranose</b></p>	1a	3.57	3.58	+0.01	$J_{1a-1b} = 12.1$
	1b	3.72	3.73	+0.01	
	3	3.81	3.80	-0.01	$J_{3-4} = 10.1$
	4	3.91	3.90	-0.01	$J_{4-5} = 3.6$
	5	4.00	4.01	+0.01	$J_{5-6a} = 1.6$ $J_{5-6b} = 2.4$
	6a	4.03	4.03	0.00	$J_{6a-6b} = 12.8$
	6b	3.72	3.72	0.00	
 <p><b><math>\beta</math>-furanose</b></p>	1a	3.56	3.56	0.00	$J_{1a-1b} = 11.9$
	1b	3.61	3.60	-0.01	
	3	4.12	4.12	0.00	$J_{3-4} = 1.0$
	4	4.12	4.13	+0.01	$J_{4-5} = 3.7$
	5	3.85	3.85	0.00	$J_{5-6a} = 3.3$ $J_{5-6b} = 6.0$
	6a	3.81	3.81	0.00	$J_{6a-6b} = 12.1$
	6b	3.68	3.70	+0.02	
 <p><b><math>\alpha</math>-furanose</b></p>	1a	3.65	/**	/	/
	1b	3.69	/	/	
	3	4.11	4.12	+0.01	$J_{3-4} = 5.2$
	4	4.01	4.02	+0.01	$J_{4-5} = 6.9$
	5	4.06	4.08	+0.02	$J_{5-6a} = 3.0$ $J_{5-6b} = 5.5$
	6a	3.82	3.84	+0.02	$J_{6a-6b} = -12.3$
	6b	3.70	3.70	0.00	

\*These values are referenced by the previous research<sup>4,5</sup>.

\*\*Compared with other tautomers, the coupled spins of H1b and H1a can't be observed in our spectrum since the extreme low concentration of  $\alpha$ f.

#### 4. Spectral foldings in CHEESE experiment

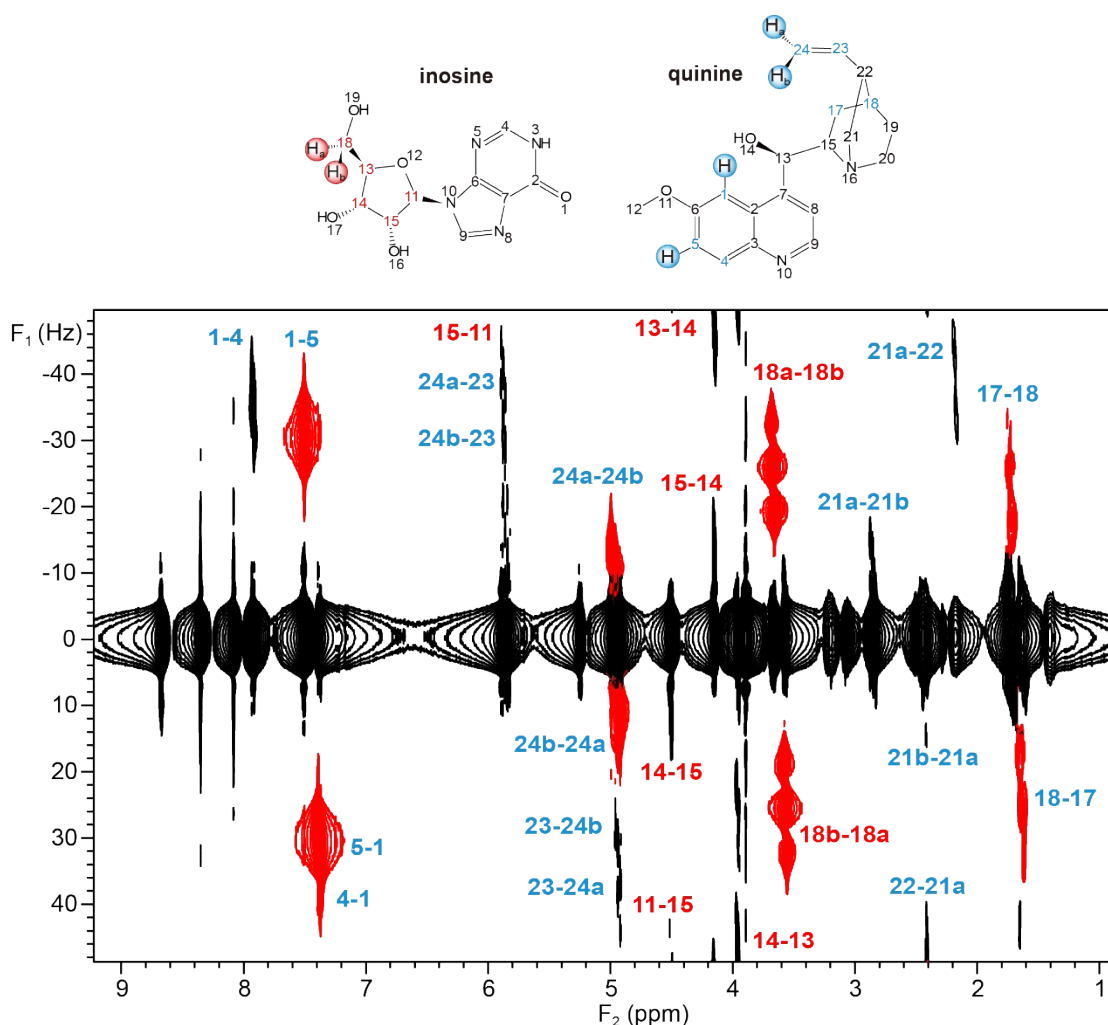


**Figure S2.** 2D CHEESE spectrum for quinine and inosine. Compared to Fig. 4c, this spectrum is plotted with contours decreased by forty times. Spectrum is apodized with the cosine bell squared function. The symbol “5-1” represents a coupling correlation network, where the active and the observed protons are H5 and H1 respectively. The folded and unfolded cross-peak multiplets are marked in red and black, respectively. The symbols corresponding to quinine and inosine are marked in blue and red, respectively.

Table S2. Chemical shift differences and the intensity of unfolded cross-peaks in Fig. S2

Unfolded cross-peaks	Chemical shift differences (Hz)	The intensity***
$H_5-H_1$	55	0.76
$H_{24b}-H_{24a}$	25	0.95
$H_{18b}-H_{18a}$	50	0.80
$H_{17}-H_{18}$	40	0.87

\*\*\* The intensity is calculated according to the expression  $\text{sinc}\left[\frac{(\Omega_S - \Omega_I)\gamma G_2 h}{2R}\right]$ , where  $R = 0.67 \text{ MHz/s}$ ,  $G_2 = 0.74 \text{ G/cm}$  and  $h = 1.5 \text{ cm}$ .

Table S3. Chemical shift differences and the intensity of folded cross-peaks in Fig. S2

<b>Folded cross-peaks</b>	<b>Chemical shift differences (Hz)</b>	<b>The intensity***</b>
H <sub>4</sub> -H <sub>1</sub>	270	-0.05
H <sub>23</sub> -H <sub>24b</sub>	455	-0.06
H <sub>23</sub> -H <sub>24a</sub>	480	0.09
H <sub>21a</sub> -H <sub>22</sub>	115	0.20
H <sub>21b</sub> -H <sub>22</sub>	335	0.13
H <sub>21b</sub> -H <sub>21a</sub>	220	-0.20
H <sub>15</sub> -H <sub>14</sub>	175	-0.18
H <sub>11</sub> -H <sub>15</sub>	690	0.02
H <sub>14</sub> -H <sub>13</sub>	100	0.36

To illustrate the effect of the spectral folding in CHEESE experiments, the contour level of spectrum shown in Fig. S2 is increased by 40 times than Fig. 4c. The CHEESE method cannot completely eliminate folded signals, but the intensities of the folded signals are weak due to large chemical shift differences. The spectral width of Fig. S2 along the  $F_1$  dimension is 100 Hz, which means that only cross peaks with less than 100 Hz chemical-shift difference are not folded. As shown in Fig. S2 and Table S2 and S3, the intensities of the unfolded cross-peak multiplets (red) are much stronger than that of the folded cross-peak multiplets (black). Furthermore, the actual intensities of cross-peaks are not only dependent on the concentrate of the component, but also on the complexity of coupled systems. Compared with the calculated intensities, the actual intensities of four- or higher-spin systems decrease dramatically, like the cross-peaks multiplets H17-H18 of quinine.

## 5. *Spinach*<sup>6</sup> codes of performing CHEESE experiment on D-fructose



```

% Sequence parameters
parameters.offset=3.79*500;
parameters.sweep=[200 500]; % Hz
parameters.npoints=[512 4096];
parameters.zerofill=[2048 8192];
parameters.spins={'1H'};
parameters.axis_units='Hz';
parameters.g_amp=0.015/2; % T/m

% Saltire chirp parameters
parameters.beta=15; % flip angle of the saltire chirp (degrees)
parameters.duration=0.015; % pulse width of saltire chirp (s)
parameters.del=0; % diffusion delay (s)
parameters.bandwidth=10000; % sweep width of saltire chirp (Hz)
parameters.pulsenpoints=100; % number of points in the saltire chirp
parameters.smfactor=20; % smoothing factor
parameters.chirptype='smoothed';

% Coherent evolution timesteps
parameters.timestep1=1/parameters.sweep(1);
parameters.timestep2=1/parameters.sweep(2);
parameters.delta=parameters.timestep1/4;

% Sample parameters
parameters.dims=0.015; % m
parameters.npts=100;
parameters.deriv={'period', 7};

% Diffusion and flow
parameters.diff=0; % m2/s
parameters.u=zeros(parameters.npts, 1);

% Initial and detection state phantoms
parameters.rho0_ph={ones(parameters.npts, 1)};
parameters.rho0_st={state(spin_system, 'Lz', '1H', 'cheap')};
parameters.coil_ph={ones(parameters.npts, 1)};
parameters.coil_st={state(spin_system, 'L-', '1H', 'cheap')};

% Relaxation phantom
parameters.rlx_ph={};
parameters.rlx_op={};

% Simulation

```

```

fid=imaging(spin_system,@CHEESE,parameters);

% Reconstructing the pure shift FID
% np_chunk=parameters.sweep(2)/parameters.sweep(1);
% fidps=fid(1:np_chunk,:); fidps=fidps(:);

% Apodization
fid=apodization(fid,'sqcosbell-2d');
% fidps=apodization(fidps,'gaussian-1d',6);

% Fourier transform
spectrum_2d=fftshift(fft2(fid,parameters.zerofill(2),...
                        parameters.zerofill(1)));
% spectrum_ps=fftshift(fft(fidps,parameters.zerofill(2)));

% Plotting: full 2D version
figure();
% subplot(1,2,1);
plot_2d(spin_system,abs(spectrum_2d),parameters,20,[0.05 1.0 0.05
1.0],2,256,6,'positive');

end

```

## 6. Pulse program codes for Varian spectrometers

```
#include <standard.h>
```

```
/* PHASECYCLE CALCULATION */
```

```
Static int ph1[4] = {0, 2, 1, 3},  
          ph2[8] = {0, 0, 1, 1, 2, 2, 3, 3};
```

```
pulsesequence()
```

```
{  
    double hsglvl = getval("hsglvl"),  
           hsgt = getval("hsgt"),  
           satpwr = getval("satpwr"),  
           satdly = getval("satdly"),  
           gzlvl3 = getval("gzlvl3"),  
           gzlvl4 = getval("gzlvl4"),  
           gtE4 = getval("gtE4"),  
           gstab = getval("gstab"),  
           tau = getval("tau"),  
           tof1 = getval("tof1"),  
           tz = getval("tz"),  
           selpwrh = getval("selpwrh"),  
           selpwh = getval("selpwh"),  
           selpwr = getval("selpwr"),  
           selpw = getval("selpw"),  
           zqfpw1 = getval("zqfpw1"),  
           zqfpwr1 = getval("zqfpwr1"),  
           gzlvlzq1 = getval("gzlvlzq1"),  
           chirppw=getval("chirppw"),  
           chirppwr=getval("chirppwr");  
  
    char  
        sspul[MAXSTR], satmode[MAXSTR], wet[MAXSTR], selpat90[MAXSTR], selpat180[MAXSTR],  
        chirp_1[MAXSTR], zqfpat1[MAXSTR], chirp_2[MAXSTR];  
    getstr("zqfpat1", zqfpat1);  
    getstr("satmode", satmode);  
    getstr("sspul", sspul);  
    getstr("wet", wet);  
    getstr("chirp_1", chirp_1);  
    getstr("chirp_2", chirp_2);  
    getstr("selpat90", selpat90);  
    getstr("selpat180", selpat180);  
    settable(t1, 4, ph1);  
    getelem(t1, ct, v1);  
    settable(t2, 8, ph2);  
    getelem(t2, ct, v2);
```



```

assign(v1, oph);

/* BEGIN ACTUAL SEQUENCE */
status(A);
  obspower(tpwr);

if (sspul[0] == 'y')
{
  zgradpulse(hsglv1, hsgt);
  rgpulse(pw, zero, rof1, rof1);
  zgradpulse(hsglv1, hsgt);
}

if (satmode[0] == 'y')
{
  if (d1 - satdly > 0)
    delay(d1 - satdly);
  else
    delay(0.02);
  obspower(satpwr);
  if (satfrq != tof)
    obsoffset(satfrq);
  rgpulse(satdly, zero, rof1, rof1);
  if (satfrq != tof)
    obsoffset(tof);
  obspower(tpwr);
  delay(10e-5);
}
else
{ delay(d1); }

if (getflag("wet"))
  wet4(zero, one);

status(B);
obsoffset(tof);
obspower(tpwr);
rgpulse(pw, v1, rof1, rof1);

delay(d2/2);

zgradpulse(gzlv14, gtE4);
delay(gstab);

```

```

rgradient('z',gzlv13);
obspower(chirppwr);
shaped_pulse(chirp_1,chirppw,v2,rof1,rof1);
shaped_pulse(chirp_2,chirppw,v2,rof1,rof1);
rgradient('z',0.0);
delay(gstab);
zgradpulse(gzlv14,gtE4);

delay(d2/2);

status(C);
}

```

## Reference

- [1] James Keeler, Understanding NMR spectroscopy, second edition. A John Wiley & Sons, Ltd Publication.
- [2] M.J. Thrippleton, Richard A.E. Edden, James Keeler, Suppression of strong coupling artefacts in *J*-spectra. *J. Magn. Reson.* 174 (2005) 97–109.
- [3] Yoav Shrot, Lucio Frydman, Spatially encoded NMR and the acquisition of 2D magnetic resonance images within a single scan. *J. Magn. Reson.* 172 (2005) 179-190.
- [4] T. Barclay, M. Ginic-Markovic, M. R. Johnston, P. Cooper, N. Petrovsky, Observation of the keto tautomer of D-fructose in D<sub>2</sub>O using <sup>1</sup>H NMR spectroscopy. *Carbohydr. Res.* 347 (2012) 136-141.
- [5] H.J. Hogben, M. Krzystyniak, G.T.P. Charnock, P.J. Hore, I. Kuprov, Spinach - A software library for simulation of spin dynamics in large spin systems. *J. Magn. Reson.* 208 (2011) 179-194.
- [6] I. Kuprov, Large-scale NMR simulations in liquid state: A tutorial. *Magn. Reson. Chem.* 56 (2018) 415-437.